arXiv:1404.0426v1 [physics.optics] 2 Apr 2014

Crystalline Whispering Gallery Mode Resonators: In Search of The Optimal Material

V. S. Ilchenko, A. A. Savchenkov, A. B. Matsko, and L. Maleki

OEwaves Inc., 465 N. Halstead Street, Suite 140, Pasadena, California, 91107, USA

ABSTRACT

Different applications of crystalline whispering gallery mode resonators call for different properties of the resonator host material. We report on our recent study of resonators made out of sapphire, diamond, and quartz crystals and discuss possible applications of these resonators. In particular, we demonstrate Kerr frequency comb generation in sapphire microresonators.

Keywords: Diamond, Sapphire, Quartz, Whispering Gallery Modes, Crystalline Microresonator, Hyper-Parametric Oscillator, RF Photonic Oscillator, Self-Injection Locked Laser;

Reprinted from: V. S. Ilchenko, A. A. Savchenkov, A. B. Matsko and L. Maleki,
"Crystalline whispering gallery mode resonators: in search of the optimal material,"
Proc. SPIE 8960, Laser Resonators, Microresonators, and Beam Control XVI, 896013 (March 4, 2014);
doi:10.1117/12.2044823; *http* : *//dx.doi.org*/10.1117/12.2044823

1. INTRODUCTION

An efficient technique of measurement of attenuation of transparent optical crystals involves fabrication of monolithic resonators out of the materials and measurement of their intrinsic quality ($Q-$) factors. The attenuation of light in the resonator mode, α, is related to the quality factor of a circular monolithic resonator as $Q = 2\pi n_0/(\lambda\alpha)$, where λ is the wavelength of measurement, and n_0 is the refractive index of the material at this wavelength. The value of coefficient α is determined by both absorption and scattering in the bulk material and on the surface of the resonator. Hence, α gives a reasonable approximation of the bulk absorption if other loss mechanisms are made negligible.

Whispering gallery mode (WGM) resonators are solid state cavities that confine light in small geometrical volumes for long periods of time.[1] These structures are promising for many applications in nonlinear optics, RF photonics, and optical technology[1] ranging from cavity QED[2] to Kerr optical frequency comb generation.[3,4] Finesse of WGM resonators can exceed the finesse of the best Fabry-Perot resonators and the linewidth of the WGMs can be as small as a few kHz at room temperature.[5]

Various properties of the resonators are required depending on particular applications. For example, planar on-chip integration of a microresonator calls for resonators with high enough index of refraction. The refractive index should exceed the refractive index of fused silica substrate and preferably approach refractive index of silicon nitride or silicon. Low index materials, like magnesium and calcium fluoride, are not suitable for this purpose. They hinders integration of Kerr frequency comb generators.[4] In this work we demonstrate, for the first time, generation of the Kerr frequency combs in sapphire resonators. Those resonators have excellent mechanical properties and represent a great potential for heterogeneous integration with photonic chips.

Ultra-stable cavities are required for laser stabilization.[6] The ultimate stability of a monolithic microresonator is limited by fundamental thermodynamic fluctuations existing even if the resonator is kept at constant temperature.[7] The thermal conductivity of the resonator host material is essential to reduce those fluctuations. In addition, resonators with high thermal conductivity are less sensitive to various kinds of thermal effects resulting from slow heat spread from the mode volume to the substrate.[9–11] In this work we report on fabrication of a diamond resonator that has extremely high thermal conductivity.[8]

Send correspondence to A.B.Matsko: Andrey.Matsko@oewaves.com

Tunability of WGM resonators is important in many applications. For instance, structures containing multiple interacting resonators require coincidence of the WGM frequencies belonging to different resonators.[12–14] The fabrication of completely identical very high-Q resonators is not practical, so the postproduction trimming as well as fast real time tuning of the resonant frequencies is required. Some crystalline WGM resonators possessing electro-optic effect can be tuned electrically.[15] However, the quality (Q) factors of those resonators are usually not very high and do not exceed one billion. Ultra-high Q WGM resonators are fabricated from amorphous or centro-symmetric crystals possessing some cubic nonlinearity and zero quadratic nonlinearity.[5] Such resonators can be tuned by either strain or heat, but cannot be efficiently electrically tuned. We demonstrate that crystalline quartz WGM resonators can bridge this gap. Quatrz resonators can simultaneously posses very high Q and be tuned electrically. We describe experimental demonstration of such resonators and discuss their properties and potential applications.[16]

In what follows we describe our results on studies of sapphire, diamond, and quartz whispering gallery mode resonators.

2. SAPPHIRE WHISPERING GALLERY MODE RESONATOR

We have fabricated sapphire whispering gallery mode resonators (Fig. 1) out of sapphire preforms and shown that pumping the resonators with continuous wave light results in generation of Kerr frequency combs (Fig. 2). The resonators have coupled Q-factor exceeding 10^9 at 1550 nm wavelength. Strong stimulated Rayleigh scattering results in splitting the WGM spectra into doublets, shown at left panel of (Fig. 1). Since sapphire has high enough index of refraction (1.74705 ordinary and 1.73924 extraordinary at 1500 nm) and is easily machinable, it is well suited for planar integration. Mid-IR transparency of the material makes it promising for generation of frequency combs in this spectral region.

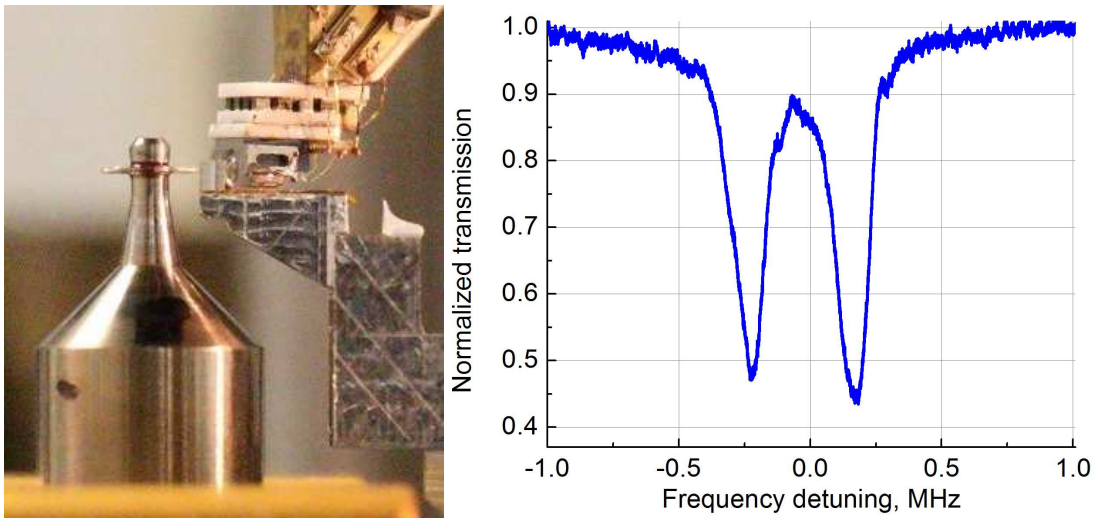

Figure 1. A picture of the sapphire resonator on a manufacture pin inserted into the test setup (left panel), and example of the optical spectrum of the resonator (right panel). A distinct 420 kHz doublet due to Rayleigh scattering is clearly seen. The WGMs have bandwidths of 160 kHz for the polarization perpendicular to the resonator axis and 260 kHz for the polarization parallel to the resonator axis.

3. DIAMOND WHISPERING GALLERY MODE RESONATOR

While it is well known that diamond has an extremely broad optical transparency window, there is little consistent experimental data on its attenuation within the window. It is relatively easy to measure transparency of fused silica because of kilometers of optical fibers fabricated from the material, however this approach is not applicable to the diamond by obvious reasons.

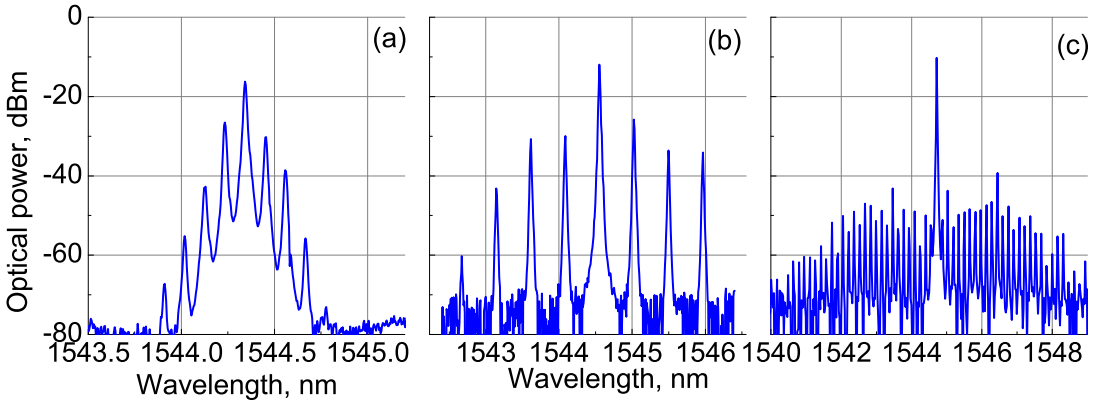

Figure 2. Examples of optical spectra of Kerr frequency combs generated in the sapphire resonator.

Methods of fabrication of high quality diamond crystals[17] has resulted in the material being used in a range of novel applications from optic to quantum information.[18–23] The material is attractive because of its exceptional physical and chemical properties, including high thermal conductivity, mechanical hardness, and a wide optical transparency window from vacuum ultraviolet through the infrared.

The best Q-factor of a monolithic diamond resonator measured at 1,550 nm, up to our knowledge, is 2.5×10^5,[24] which corresponds to linear attenuation coefficient $\alpha \simeq 0.4$ cm^{-1}. The measurements were performed with a single crystal diamond race-track resonator built on top of a silicon dioxide/silicon substrate. Observations have included the splitting of relatively low Q resonances due to stimulated Rayleigh scattering, hence we can conclude that the experimentally measured Q values are not limited by the bulk loss of the material. The scattering usually results from roughness of the surface of open microresonators. Mechanical polishing allows reaching outstanding surface quality that already lead to demonstration of the highest finesse monolithic resonators ($\mathcal{F} > 10^7$,[5]). We used this technique to fabricate a diamond resonator.[8] The measured quality factor of the resonator was $Q = 2.4\times10^7$, which is two orders of magnitude larger compared with the best previous measurement. We found that in our case the measured Q-factor is limited by the material loss approaching $\alpha = 4\times10^{-3}$ cm^{-1} and not by surface scattering.

The single-crystal diamond samples used in this experiment were synthesized with a microwave plasma-assisted chemical vapor deposition reactor operating at a frequency of 896 MHz. The sample was produced from homo-epitaxial layer grown on a $\langle 1,0,0\rangle$-orientated diamond surface that had been prepared using high quality polishing techniques to minimize Ra (<20 nm) and therefore reduce the nucleation of dislocations in the epitaxial layer.

The diamond that had approximately 20 ppb of nitrogen impurities in the solid, which results in extremely low levels of absorption across the whole transparency spectrum.[22] This kind of a diamond was utilize to build the WGM resonator. Diamond parts for quantum computing applications have been produced in thin layers with nitrogen impurities below 1 ppb,[21] and it can be foreseen that using the techniques exploited in the synthesis of these layers that in the future even lower absorption bulk diamond can be produced.

The fabricated resonator is shown in Fig. (3). It is shaped as a sphere with the diameter of $2a = 2$ mm,truncated about 130 micron below large diameter ("equatorial plane") and suspended on a metallic rod during fabrication and measurement. Refractive index of diamond is $n_0 = 2.386$ at 1,550 nm.

Measurement of the Q-factor was done by means of the prism coupling method. We used a silicon prism (refractive index $n_p = 3.48$) to couple light in and out of the resonator modes. The ultimate coupling efficiency achieved in the experiment exceeds 70%. A tunable fiber laser was utilized as a pumping light source. The linewidth of the emitted light (< 4 kHz) was small enough to perform spectroscopy of the resonator modes. A typical measured spectrum is shown in Fig. 4. The intrinsic Q-factor was inferred from the measurement of the bandwidth of the observed resonances in the undercoupled regime.

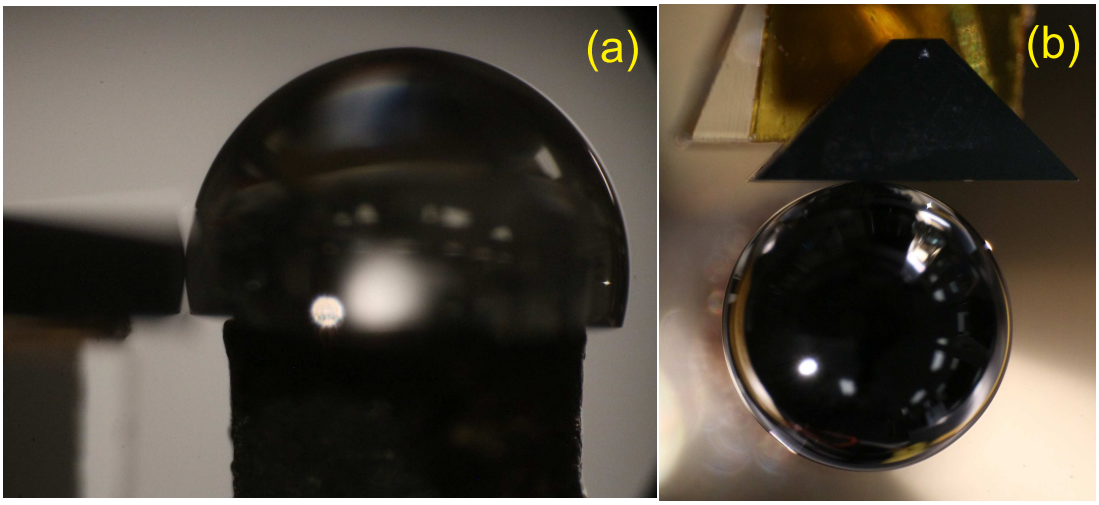

Figure 3. Pictures of the fabricated diamond whispering gallery mode resonator: (a) side view, (b) top view. A silicon prism is used to couple light in and out of the resonator.

The modes are characterized with unloaded full width at the half maximum of $8 - 10$ MHz. A general criterion to distinguish surface and bulk attenuation in the open optical resonators is the equivalence of the unloaded quality factors of all the resonator modes independently on their polarization. The modes polarized along the symmetry axis have slightly worse Q-factor (less than 10%), which indicates that the surface of the resonator is either slightly damaged or contaminated. Visual inspection has indicated presence of the minor residual scratches that can explain the slight difference in the Q-factors because of different impact of surface scattering on Q of WGMs with different polarization.

Nearly the same Q-factor was measured at 1319 nm wavelength using diode pumped Nd:YAG solid state laser. The laser light had 100 kHz linewidth. It was coupled to the resonator using the same coupling prism. This measurement shows that the attenuation is rather broadband.

The spectrum of the resonator has distinct azimuthal and latitudinal spectral features, which indicates that the resonator has a slightly spheroidal shape. The azimuthal free spectral range is 20 GHz. The latitudinal spectral range depends on the polarization of the modes. It is 263 MHz for the modes polarized collinearly with the symmetry axis of the resonator, and 249 MHz for the modes polarized perpendicularly to the axis. We were able to optimize the coupling with the higher order modes by changing the launch angle for the beam of the pumping light impinging on the resonator surface.

A spheroidal resonator has two nearly equidistant mode sequences characterized with frequency intervals

$$FSR_1 = \frac{c}{2\pi n_0 a} \tag{1}$$

and

$$FSR_2 = FSR_1 \frac{a-b}{b} \tag{2}$$

a and b are the semi-axes of the spheroid.[25–28] Using result of our measurement we conclude that non-sphericity of the resonator is approximately 1% ($(a-b)/b \simeq 0.014$).

Thermal nonlinearity is an important factor that limits the optical power range in applications of high-Q resonators.[9–11] The easily observed manifestation of thermal nonlinearity is the visible extension (or compression) of WGM resonances observed during sweeping the probe laser: because of the thermal nonlinearity, the trace of the resonance on the screen of oscilloscope changes depending on the laser power and the speed and direction of the laser frequency scan. This effect is produced by heating the mode volume with the light power absorbed in the material due to nonzero optical absorption. The process can be described with two time constants, one of which is responsible for flow of heat from the mode volume to the rest of the resonator, and the other – for

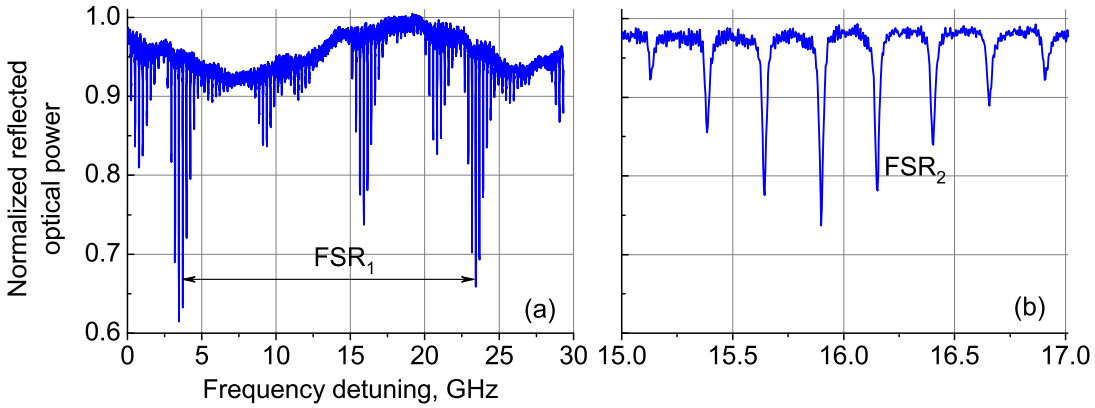

Figure 4. Spectrum of the resonator modes polarized perpendicular to the resonator symmetry axis. Two free spectral ranges (FSRs)are observed. FSR_1 corresponds to azimuthal quantization of the modes, FSR_2 corresponds to altitudinal quantization of the modes.

heat exchange between the resonator and external environment. The laser scan should be fast compared with the relaxation constants and the light power must be small to reduce the effect.

In the simplest approximation the evolution of the system can be described with a set of two equations[11]

$$\dot{E} + [\gamma + i\,(\omega - \omega_0 + \delta)]\,E = F(t),$$
$$\dot{\delta} + \Gamma\delta = \Gamma\gamma\xi|E|^2,$$

where E is the complex amplitude of the field in the resonator mode normalized such that $|E|^2$ is the total energy accumulated in the mode, γ is the optical mode half width at the half maximum, ω is the frequency of the optical pump, ω_0 is the unperturbed resonance eigenfrequency, $\delta = \omega_0\beta\Delta T$ is the thermal frequency shift, $\beta = (1/n_0)(\partial n_0/\partial T)$, ΔT is the temperature deviation, $F(t)$ stands for the external optical pump, $\Gamma = 2D/h^2$ characterizes thermal relaxation rate, $D = \lambda^*/(\rho C)$ is thermal diffusivity, λ^* is thermal conductivity, ρ is material density, C is a specific heat capacity of diamond, h is the half-thickness of the mode in the direction of the largest field gradient, which is the radial direction for the spherical resonator; and

$$\xi = \frac{\omega_0\beta n_0^2 h^2}{8\pi\lambda^* V_{eff}}\frac{Q}{Q_{abs}} \tag{3}$$

is the thermal nonlinearity coefficient, where Q_{abs} is the quality factor determined by the material absorption. The thermal nonlinearity becomes important when the power accumulated in the resonator exceeds ξ^{-1}. It is easy to see from Eq. (3) that thermal nonlinearity of a diamond resonator is very small compared with the thermal nonlinearity of other optical materials, since the thermal conductivity in diamond is significantly larger compared with thermal conductivity of any other optical crystal.

To confirm the conclusion we performed a comparative measurement of thermal nonlinearity of two identical resonators. One of the resonators was the diamond one, and the other was made with MgF_2. The MgF_2 resonator was fabricated so that its Q_{abs} was comparable with the Q of the diamond resonator. In this case $\xi_{MgF2}/\xi_{diamond} \simeq 360$. It means that thermal nonlinearity becomes visible in magnesium fluoride for pump power hundred times smaller compared with the identical diamond resonator.

The thermal nonlinearity can be significantly suppressed if the resonators of high transparency material are overloaded in such a way that the loaded Q becomes much smaller than the absorption-related Q_{abs} ($Q_{abs} \gg Q$). If one is able to maintain extremely low levels of absorption in a resonator with transparent material with Q_{abs} much larger than the one of diamond, as in the case of CaF_2[5] and MgF_2, the benefit of diamond as extreme thermal conductivity material could become irrelevant. This, however, is a challenging engineering task, since not only the resonator material must have ultra-low loss, but absorptive contaminations must also be avoided during integration of the resonator.

The diamond resonators have an important advantage compared with resonators of other materials if the goal is to create an ultra-stable cavity. The ultimate stability of monolithic resonators is limited by fundamental thermodynamic fluctuations existing even if the resonator is kept at constant temperature. For instance, thermodynamic fluctuation of temperature in the mode volume results in fluctuations of the index of refraction in the mode channel that can be written as[7]

$$\left.\frac{\Delta n}{n}\right|_{(\Delta T)_m} = \beta(\Delta T)_m. \tag{4}$$

The mean square value of the temperature fluctuation is

$$\langle (\Delta T)_m^2 \rangle = \frac{k_B T^2}{C\rho V_{eff}}, \tag{5}$$

where k_B is the Boltzmann's constant, T is the absolute temperature.

The spectral power density of the fluctuation of the averaged temperature of the mode of a toroidal resonator ($\bar{T}(t)$) is[7]

$$S_{\bar{T}}(\Omega) \approx \frac{k_B T^2 a^2}{12\lambda^* V_{eff}} \left[1 + \left(\frac{a^2}{D}\frac{|\Omega|}{9\sqrt{3}}\right)^{3/2}\right]^{-1}. \tag{6}$$

The spectral density is inversely proportional to the thermal conductivity of the resonator host material. Therefore, the thermorefractive noise will be significantly smaller in a diamond resonator. The thermal fluctuation does not depend on the loss of the resonator host material. It shows that the existing resonator already has certain advantages over other, higher-Q, crystalline resonators.

4. CRYSTALLINE QUARTZ WHISPERING GALLERY MODE RESONATOR

By adapting the mechanical polishing technique we have developed, we fabricated quartz WGM resonators[16] out of cylindrical crystal quartz preforms purchased from two different vendors. The mechanical polishing was realized with a diamond slurry. The polishing quality is high enough to ensure negligible surface scattering of light traveling in the WGMs. Extremity of the resonators is shaped into toroidal geometry.

Modes in the resonators were excited using a SF11 prism coupler and a 1550 nm tunable fiber laser having 4 kHz linewidth. The modes with quality factors approaching $Q = 5 \times 10^9$ (see Fig. 5a) were detected in z-cut resonators (the symmetry axis of the resonators coincides with the z-axis of quartz).

Because of the crystalline properties a Z-cut quartz resonator is not tunable by an electric field applied along its symmetry axis. We placed metal electrodes on the top and bottom surfaces of a 100 μm thick resonator and applied a DC voltage (as done in[15]). No measurable voltage-dependent mode shift was observed for the voltage amplitude exceeding 200 V.

To observe the electric tunability of the WGM spectrum we fabricated resonators out of x-cut quartz. The optical quality of the x-cut crystal quartz samples in our disposal was not good enough so the maximum Q-factor of those resonators was an order of magnitude lower than that of the z-cut resonators.

We have measured the value of the Pockels constant of quartz (first measured by Pockels himself[29–31]) by applying a DC voltage to the x-cut resonator's top and bottom surfaces and measuring the frequency shift of the WGMs.[15] For instance, the TE mode family shifts by $\delta\nu = 78$ MHz when we apply $V = 133$ V to the $h = 220$ μm thick disk, so that $r_{11} = 2\delta\nu h/(V\nu n^2)$, where $\nu = 1.94 \times 10^{14}$ Hz is the carrier frequency of the pump light and $n = 1.53$ is the index of refraction of the material at 1550 nm. The measured value is $r_{11} = 0.57$ pm/V. Interestingly, not only TE, but also TM modes experience frequency shifts when the electric field is applied. This basically means that the modes in our resonator do not have the distinct parallel or orthogonal direction of the electric field with respect to the symmetry axis of the resonator.

Electrical tunability of quartz WGM resonators enables WGM electro-optical modulators[32,33] (feasibility of quartz electro-optical modulators have been noted previously[34–36]). We have fabricated such a modulator using

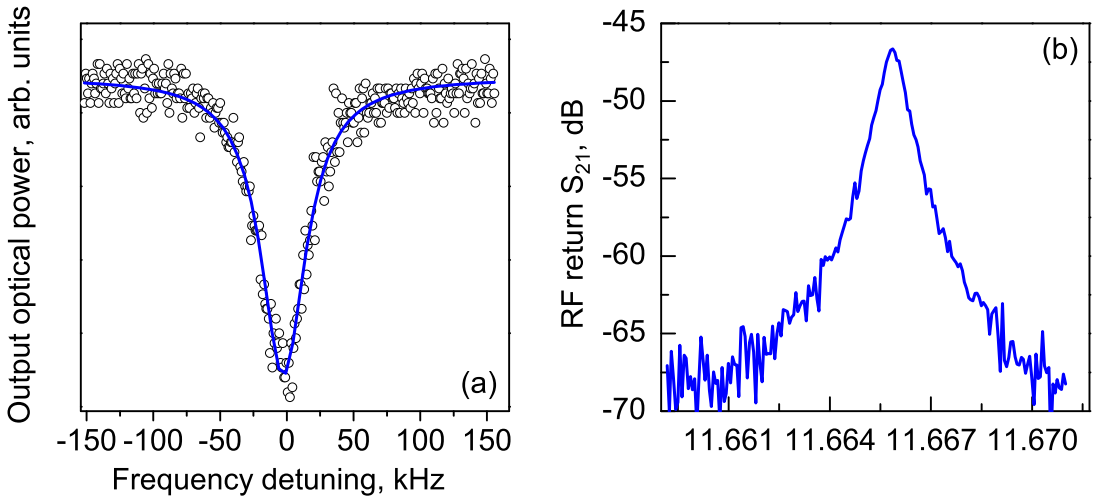

Figure 5. (a) A WGM resonance belonging to a z-cut quartz WGM resonator. Solid line is a Lorentzian fit to the experimental data. The optical power sent to the mode is small enough ($P_{in} = 3$ μW) to avoid nonlinear processes. The linewidth corresponds to $Q = 5 \times 10^9$. (b) RF return for the modulator based on the X-cut quartz resonator versus RF modulation frequency (the ratio of the powers of the demodulated signal and the input signal). The input microwave as well as the optical power at the high speed photodetector is equal to 1 mW. The RF return frequency bandwidth is ~ 0.8 MHz at -3 dB. The loaded quality factor of the optically pumped WGM is $Q = 2 \times 10^8$ (optical bandwidth is 1 MHz). The optical mode contrast is 50%. The laser is manually tuned to the mode. The maximum RF return corresponds to $S_{21} \simeq 2 \times 10^{-5}$.

a standard technique utilized previously with lithium-niobate WGM modulators.[33] We mounted a strip line RF resonator on top of the resonator sitting on a polished brass electrode, and tuned the RF resonance frequency such that it became identical to the free spectral range (FSR) of the optical resonator. The strip line was placed at the resonator circumference to ensure an overlap between the RF field and the light confined in the modes. The resultant RF strip line resonator covered approximately 190^o of the WGM resonator perimeter. The full width at the half maximum (FWHM) of the RF mode was 215 MHz, the RF resonant frequency was 11.7 GHz, hence the RF quality factor was $Q_{RF} \simeq 54$.

To operate the modulator we sent laser radiation to a WGM and a continuous wave RF signal to the strip line resonator. The nonzero r_{11} of quartz ensures the wave mixing process between light and the RF signal. The wave mixing results in generation of optical sidebands resonant with the optical modes separated from the pumped WGM by an integer number of FSRs. The first order sidebands grow first, followed by the higher order sidebands. We demodulated the light escaping the resonator by means of a fast photodiode and observed the RF signal using an RF spectrum analyzer (Fig. 5b). It is possible to find the parameters of the modulator using this signal.

The RF return of the modulator can be expressed as[33]

$$S_{21} = \xi \frac{\rho_{pd} \mathcal{R}^2 P_{in}^2}{P_{sat}}, \tag{7}$$

$$P_{sat} = \frac{n_{RF}^2 \omega_{RF} \mathcal{V}_{RF}}{8\pi Q^2 Q_{RF} r_{11}^2 n^4 \eta^2}, \tag{8}$$

where $1 > \xi > 0$ is the numerical parameter taking into account the coupling efficiency of the light into the resonator as well as the type of the modulation (an all-resonant modulator produces mostly phase modulated light zeroing down S_{21}), P_{sat} is the RF saturation power of the modulator, ρ_{pd} is the resistivity of the photodiode, $\mathcal{R}$ is the responsivity of the photodiode, P_{in} is the power of the light, Q and Q_{RF} are the quality factors of the optical and microwave modes, r_{11} is the electro-optical coefficient of the resonator host material, n and n_{RF} are the indices of refraction of the material, $\mathcal{V}_{RF}$ is the volume of the microwave field, $\eta = (1/V_e) \int |\Psi_e|^2 \Psi_{RF} dV < 1$

is the overlap integral of the optical and microwave fields, $|\Psi_e|^2$ and $|\Psi_{RF}|^2$ are the spatial distributions of the power of the optical and microwave fields respectively, $(1/V_e)\int |\Psi_e|^2 dV = 1$, and ω_{RF} if the RF frequency.

To find the saturation power we use $Q = 2 \times 10^8$, $Q_{RF} = 54$, $\omega_M = 2\pi \times 11$ GHz, $\eta = 0.5$, $r_{11} = 0.57$ pm/V$=1.3 \times 10^{-9}$ esu, $n_e = 1.53$, $n_{RF} = 2.15$, $\mathcal{V}_{RF} = 2 \times 10^{-4}$ cm^3 (the volume is given by the 100 μ wide strip line resonator having πR length and 220 μm thickness). Then we estimate $P_{sat} \simeq 51$ mW. We also know from the experiment that $S_{21} \simeq 2 \times 10^{-5}$, $P_{in} = 1$ mW, $\rho_{pd} = 50$ Ohm, and $\mathcal{R} = 0.8$ A/W. Using these values and the calculated value for the saturation pump power we obtain $\xi = 4 \times 10^{-2}$. Because ξ is small our modulator generate mostly phase modulated light.

The electro-optical modulator based on the quartz WGM resonator will become extremely important if the quality factor of the optical resonator fabricated from the x-cut material can be significantly increased. This will cause the saturation power of such a resonator to be low, so the modulation will be very efficient. The modulator will then also have an extremely narrow bandwidth. Such properties are important in harmonically mode locked lasers[37,38] and coupled opto-electronic oscillators.[39] Indeed, optical etalons have been inserted into the optical loop to improve the performance of harmonically actively mode-locked lasers,[37,38] and electro-optical modulators are the key parts of those lasers. The quartz WGM modulator is able to substitute both the modulator and the etalon in the mode-locked lasers. The low saturation power of quartz modulator will eliminate the requirement of high power RF amplifiers in oscillators, while the narrow filter function will reduce the phase noise.

A laser locked to a narrow resonance high-finesse resonator is the commonly used source of stable narrow-linewidth optical signals. Extremely narrow linewidth of the WGMs in quartz resonators will allow realizing lasers with high short-term stability, while electro-optical tunability of the WGM will allow tuning or modulating the frequency of the lasers.

Finally, let us discuss the nonlinear optical properties of the quartz resonators. It is known that quartz has several Raman lines[40–42] and possesses a large cubic nonlinearity ($n_2 = 1.7 \times 10^{-14}$ esu, 1.4 times larger than fused silica[43,44]). Therefore, we should expect to observe stimulated Raman scattering (SRS) as well as four-wave mixing in the quartz resonators as previously observed in fused silica resonators. To examine this, we amplified our laser and pumped the quartz resonators with 40 mW light. The only effect observed was the SRS. No hyper-parametric oscillations based on four-wave mixing were detected. The reason for the suppression of the effects will be the subject of further investigations.

5. CONCLUSION

We have presented results concerning fabrication of high-Q sapphire, diamond, and crystal quartz whispering gallery mode resonators, and demonstrated the highest reported Q-factor in a monolithic resonators fabricated out of the materials. The resonators can be useful in a variety of scientific and technical applications, including fabrication of ultra-stable optical etalons, cavity-stabilized lasers, and opto-electronic radio-frequency oscillators.

Acknowledgments

The authors acknowledge support from Defense Sciences Office of Defense Advanced Research Projects Agency under contract No. W911QX-12-C-0067 as well as support from Air Force Office of Scientific Research under contract No. FA9550-12-C-0068.

REFERENCES

1. V. S. Ilchenko and A. B. Matsko, "Optical resonators with whispering gallery modes II: Applications," IEEE J. Sel. Top. Quantum Electron. **12**, 15-32 (2005).
2. T. Aoki, B. Dayan, E. Wilcut, W. P. Bowen, A. S. Parkins, T. J. Kippenberg, K. J. Vahala, H. J. Kimble, "Observation of strong coupling between one atom and a monolithic microresonator," Nature **443**, 671-674 (2006).
3. P. Del Haye, A. Schliesser, O. Arcizet, T. Wilkins, R. Holzwarth, T. J. Kippenberg, "Optical frequency comb generation from a monolithic microresonator," Nature **450**, 1214-1217 (2007).

4. A. A. Savchenkov, A. B. Matsko, V. S. Ilchenko, I. Solomatine, D. Seidel, and L. Maleki, "Tunable optical frequency comb with a crystalline whispering gallery mode resonator," Phys. Rev. Lett. **101**, 093902 (2008).
5. A. A. Savchenkov, A. B. Matsko, V. S. Ilchenko, and L. Maleki, "Optical resonators with ten million finesse," Opt. Express **15**, 6768-6773 (2007).
6. W. Liang, V. S. Ilchenko, A. A. Savchenkov, A. B. Matsko, D. Seidel, and L. Maleki, "Whispering-gallery-mode-resonator-based ultranarrow linewidth external-cavity semiconductor laser," Opt. Lett. **35**, 2822–2824 (2010).
7. A. B. Matsko, A. A. Savchenkov, N. Yu, and L. Maleki, "Whispering-gallery-mode resonators as frequency references. I. Fundamental limitations," J. Opt. Soc. Am. B **24**, 1324-1335 (2007).
8. V. S. Ilchenko, A. M. Bennett, P. Santini, A. A. Savchenkov, A. B. Matsko, and L. Maleki, "Whispering gallery mode diamond resonator," Opt. Lett. **38**, 4320-4323 (2013).
9. M. L. Gorodetsky and V. S. Ilchenko, "Thermal nonlinear effects in optical whispering-gallery microresonators," Laser Phys. **2**, 1004-1009 (1992).
10. T. Carmon, L. Yang, and K. Vahala, "Dynamical thermal behavior and thermal self-stability of microcavities," Opt. Express **12**, 4742-4750 (2004).
11. A. E. Fomin, M. L. Gorodetsky, I. S. Grudinin, and V. S. Ilchenko, "Nonstationary nonlinear effects in optical microspheres," J. Opt. Soc. Am. B **22**, 459-465 (2005).
12. V. N. Astratov, J. P. Franchak, and S. P. Ashili, "Optical coupling and transport phenomena in chains of spherical dielectric microresonators with size disorder," Appl. Phys. Lett. **85**, 5508-5510 (2004).
13. J. K. Poon, L. Zhu, G. A. DeRose, and A. Yariv, "Transmission and group delay of microring coupled-resonator optical waveguides," Opt. Lett. **31**, 456-458 (2006).
14. S. Mookherjea and A. Oh, "Effect of disorder on slow light velocity in optical slow-wave structures," Opt. Lett. **32**, 289-291 (2007).
15. A. A. Savchenkov, V. S. Ilchenko, A. B. Matsko and L. Maleki, "Tunable filter based on whispering gallery modes", Electron. Lett. **39**, 389-391 (2003).
16. V. S. Ilchenko, A. A. Savchenkov, J. Byrd, I. Solomatine, A. B Matsko, D. Seidel, and L. Maleki, "Crystal quartz optical whispering-gallery resonators," Opt. Lett. **33**, 1569-1571 (2008).
17. K. E. Spear and J. P. Dismukes, *Synthetic diamond: emerging CVD science and technology,* (Wiley, NY, 1994).
18. A. Tallaire, A. T. Collins, D. Charles, J. Achard, R. Sussmann, A. Gicquel, M. E. Newton, A. M. Edmonds, and R. J. Cruddace, "Characterization of high-quality thick single-crystal diamond grown by CVD with a low nitrogen addition," Diamond and Related Materials **15**, 1700-1707 (2006).
19. D. D. Awschalom, R. Epstein, and R. Hanson, "The diamond age of spintronics," Sci. Am. **297**, 8491 (2007).
20. R. S. Balmer, J. R. Brandon, S. L. Clewes, H. K. Dhillon, J. M. Dodson, I. Friel, P. N. Inglis, T. D. Madgwick, M. L. Markham, T. P. Mollart, N. Perkins, G. A. Scarsbrook, D. J. Twitchen, A. J. Whitehead, J. J. Wilman, and S. M. Woollard, "Chemical vapour deposition synthetic diamond: Materials, technology and applications," J. Phys. Condens. Mat. **21**, 364221 (2009).
21. G. Balasubramanian, P. Neumann, D. Twitchen, M. Markham, R. Kolesov, N. Mizuochi, J. Isoya, J. Achard, J. Beck, J. Tissler, V. Jacques, P. Hemmer, F. Jelezko and J. Wrachtrup, "Ultralong spin coherence time in isotopically engineered diamond," Nature Materials **8**, 383-387 (2009).
22. I. Friel, S. Geoghegan, D. Twitchen, and G. Scarsbrook, "Development of high quality single crystal diamond for novel laser applications," SPIE Proc. **7838**, 783819 (2010).
23. I. Aharonovich, A. D. Greentree, and S. Prawer, "Diamond photonics," Nature Photonics **5**, 397-405 (2011).
24. B. J. M. Hausmann, I. B. Bulu, P. B. Deotare, M. McCutcheon, V. Venkataraman, M.L. Markham, D. J. Twitchen, and M. Loncar, "Integrated high quality factor optical resonators in diamond," Nano Lett. **13**, 18981902 (2013).
25. M. Sumetsky, "Whispering-gallery-bottle microcavities: the three-dimensional etalon," Opt. Lett. **29**, 8-10 (2004).
26. Y. Louyer, D. Meschede, and A. Rauschenbeutel, "Tunable whispering-gallery-mode resonators for cavity quantum electrodynamics," Phys. Rev. A **72**, 031801(R) (2005).

27. M. L. Gorodetsky, A. E. Fomin, "Geometrical theory of whispering gallery modes," IEEE J. Sel. Top. Quantum Electron. **12**, 33-39 (2006).
28. M. Pöllinger, D. O'Shea, F. Warken, A. Rauschenbeutel, "Ultrahigh-Q tunable whispering-gallery-mode microresonator," Phys. Rev. Lett. **103**, 053901 (2009).
29. F. Pockels, Abhandl. ges. Wiss., Gottingen "Ueber den Einfluss des elektrostatischen Feldes auf das optische Verhalten piëzoelektrischer Krystalle," **39**, 1 (1894).
30. W. G. Cady, *Piezoelectricity* (McGraw-Hill Book Co., New York, 1946), p. 721.
31. R. D. Rosner, E. H. Turner, and I. P. Kaminow, "Clamped electrooptic coefficients of KDP and quartz," Appl. Opt. **6**, 778-778 (1967).
32. D. A. Cohen, M. Hossein-Zadeh, and A. F. J. Levi, "High-Q microphotonic electro-optic modulator," Solid State Electron. **45**, 1577-1589 (2001).
33. V. S. Ilchenko, A. A. Savchenkov, A. B. Matsko, and L. Maleki, "Whispering gallery mode electro-optic modulator and photonic microwave receiver," J. Opt. Soc. Am. B **20**, 333-342 (2003).
34. D. D. Eden and G. H. Thiess, "Measurement of the direct electro-optic effect in quartz at UHF," Appl. Opt. **2** 868-869 (1963).
35. I. P. Kaminow and E. H. Turner, "Electrooptic light modulators," Appl. Opt. **5**, 1612-1628 (1966).
36. H. Pursey and R. J. Newman, "Measurement of the Pockels effect in quartz at 9 GHz," J. Phys. D **1**, 707 (1968).
37. G. T. Harvey and L. F. Mollenauer, "Harmonically mode-locked fiber ring laser with an internal Fabry - Perot stabilizer for soliton transmission," Opt. Lett. **18**, 107-109 (1993).
38. S. Gee, F. Quinlan, S. Ozharar, and P. J. Delfyett, "Simultaneous optical comb frequency stabilization and super-mode noise suppression of harmonically mode-locked semiconductor ring laser using an intracavity etalon," IEEE Photon. Technol. Lett. **17**, 199-201 (2005).
39. X. S. Yao and L. Maleki, "Dual microwave and optical oscillator," Opt. Lett. **22**, 1867-1869 (1997).
40. P. E. Tannenwald and J. B. Thaxter, "Stimulated Brillouin and Raman scattering in quartz at 2.1^o to 293^o Kelvin," Science **154**, 1319-1320 (1966).
41. J. F. Scott and S. P. S. Porto, "Longitudinal and transverse optical lattice vibrations in quartz," Phys. Rev. **161**, 903-910 (1967).
42. R. J. Briggs and A. K. Ramdas, "Piezo-spectroscopy of the Raman spectrum of α-quartz," Phys. Rev. B **16**, 3815-3826 (1977).
43. P. D. Maker and R. W. Terhune, "Study of optical effects due to an induced polarization third order in the electric field strength," Phys. Rev. **137**, A801-A818 (1965).
44. G. R. Meredith, "Cascading in optical third-harmonic generation by crystalline quartz," Phys. Rev. B **24**, 5522-5532 (1981).